

ISSN: 0095-8972 (Print) 1029-0389 (Online) Journal homepage: <http://www.tandfonline.com/loi/gcoo20>

Assembly of 1-D and decanuclear cage compounds from copper halide, cyclohexenephosphonic acid, and 3-(2-pyridyl)pyrazole

Yun-sheng Ma, Zhen Yang, Wang-Shui Cai, Xiao-Yan Tang & Rong-Xin Yuan

To cite this article: Yun-sheng Ma, Zhen Yang, Wang-Shui Cai, Xiao-Yan Tang & Rong-Xin Yuan (2015) Assembly of 1-D and decanuclear cage compounds from copper halide, cyclohexenephosphonic acid, and 3-(2-pyridyl)pyrazole, *Journal of Coordination Chemistry*, 68:9, 1633-1643, DOI: [10.1080/00958972.2015.1021342](https://doi.org/10.1080/00958972.2015.1021342)

To link to this article: <http://dx.doi.org/10.1080/00958972.2015.1021342>




View supplementary material 



Accepted author version posted online: 23 Feb 2015.
Published online: 16 Mar 2015.




Submit your article to this journal 



Article views: 43



View related articles 



View Crossmark data 



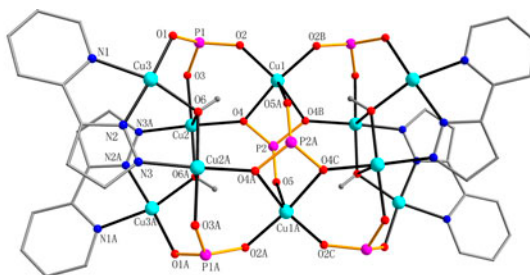
Citing articles: 1 View citing articles 

Assembly of 1-D and decanuclear cage compounds from copper halide, cyclohexenephosphonic acid, and 3-(2-pyridyl)pyrazole

YUN-SHENG MA*, ZHEN YANG, WANG-SHUI CAI, XIAO-YAN TANG and RONG-XIN YUAN

School of Chemistry and Materials Engineering, Jiangsu Key Laboratory of Advanced Functional Materials, Changshu Institute of Technology, Changshu, PR China

(Received 12 August 2013; accepted 30 January 2015)



The reactions of cyclohexenephosphonic acid ($\text{C}_6\text{H}_9\text{PO}_3\text{H}_2$) and 3-(2-pyridyl)pyrazole (2-pyPzH) with copper(II) chloride and copper(II) bromide affords a 1-D compound $[\text{Cu}(2\text{-pyPz})\text{Cl}]$ (**1**) and a decanuclear $[\text{Cu}_{10}(\text{OH})_4(\text{C}_6\text{H}_9\text{PO}_3)_6(2\text{-pyPz})_4]$ (**2**) cage complex. In **1**, adjacent copper ions are bridged by two 2-pyPz ligands into dimers, which are further linked by Cl^- into a ladder-like chain. Compound **2** has a decanuclear cage structure, the overall cage can be viewed as composed of two $\text{Cu}_4(\text{OH})_2(2\text{-pyPz})_2$ wings that are bridged by a central $\text{Cu}_2\text{P}_2\text{O}_6$ rim. Variable-temperature magnetic susceptibility studies indicate that both compounds show antiferromagnetic interactions between copper centers.

Keywords: Copper phosphonate; Cage complexes; Magnetic property

1. Introduction

Metal phosphonates have received attention for their potential applications in sorption, optics, catalysis, proton conductivity, and magnetism [1]. To search single-molecule magnets [2] or low-temperature magnetic refrigerants [3], coordination clusters featuring

*Corresponding author. Email: myschem@cslg.edu.cn

phosphonate ligands (RPO_3H_2 , R = alkyl or aryl) were investigated to take advantage of strong coordination abilities of three phosphonate oxygens. There are three methods to get discrete metal phosphonate clusters. One approach is to use ancillary ligands such as pyrazole or 6-chloro-2-hydroxy-pyridine (Hchp) to increase the solubility of the copper/cobalt phosphonates [4]. Adopting this method, Chandrasekhar and Kingsley obtained different types of copper phosphonate clusters by changing the substitution on the pyrazole ligands [5]. The second approach utilizes phosphonate ligands and preformed triangles $[\text{M}_3\text{O}(\text{O}_2\text{CR})_6(\text{py})_2(\text{H}_2\text{O})]^{0,+}$ (M = Fe, Mn; R = CH_3 , Ph) under milder reaction conditions to result in Fe4, Fe7, Fe9, and Mn22 cluster complexes [6]. The last one is a straightforward method, in which the bulkier phosphonate ligands react with simple divalent transition metal ions to produce higher nuclearity metal phosphonates, for example, Mn4, Mn5, and Mn12 [7]. The flexibility of the alkyl or aryl group attached to phosphorus could tune the nuclearities of the final clusters.

Cyclohexenephosphonic acid ($\text{C}_6\text{H}_9\text{PO}_3\text{H}_2$) has proved to be a very good ligand for iron, manganese, and cobalt phosphonate clusters [8] and has been used to construct the layered compound $[\text{Cu}(\text{C}_6\text{H}_9\text{PO}_3)(\text{H}_2\text{O})]$ [9]. To obtain new copper cyclohexenephosphonate clusters, we used 2-pyPzH as coligand to react with copper halide. Herein, we reported the synthesis and structural characterization of two copper complexes, 1-D chain **1** and decanuclear **2**, respectively.

2. Experimental

2.1. Materials and methods

All the starting materials were of reagent grade and used as purchased. Cyclohexenephosphonic acid was prepared according to the literature method [10]. Elemental analyses were performed on a PE 240C elemental analyzer. FT-IR spectra were recorded on a NICOLET 380 spectrometer with pressed KBr pellets. All the magnetic studies were performed on microcrystalline samples. The magnetic susceptibilities were measured on a Quantum Design MPMS SQUID-XL7 magnetometer. Diamagnetic corrections were made for both the sample holder and the compound estimated from Pascal's constants [11].

2.2. Syntheses

2.2.1. $[\text{Cu}(\text{2-pyPz})\text{Cl}]$ (1**).** $\text{CuCl}_2 \cdot 6\text{H}_2\text{O}$ (0.1705 g, 1 mM) was dissolved in CH_3OH (10 mL), to which was added 2-pyPzH (0.0725 g, 0.5 mM), $\text{C}_6\text{H}_9\text{PO}_3\text{H}_2$ (0.081 g, 0.5 mM), and Et_3N (0.208 mL, 1.5 mM). The reaction mixture was stirred at room temperature for 20 h. The resulting green precipitate was collected by filtration and recrystallized from DMF. Green crystals of **1** formed after one week. Yield: 0.109 g, 89.6% based on 2-pyPzH. Elemental analysis Calc. (%) for $\text{C}_8\text{H}_6\text{ClCuN}_3$: C, 39.52; H, 2.49; N, 17.28. Found: C, 39.22; H, 2.15; N, 17.01. IR (KBr, cm^{-1}): 1612m, 1454m, 1400s, 753m, 520w.

2.2.2. $[\text{Cu}_{10}(\text{OH})_4(\text{C}_6\text{H}_9\text{PO}_3)_6(\text{2-pyPz})_4] \cdot 4\text{H}_2\text{O}$ (2**).** CuBr_2 (0.223 g, 1 mM) was dissolved in CH_3OH (10 mL), to which was added 2-pyPzH (0.0725 g, 0.5 mM), $\text{C}_6\text{H}_9\text{PO}_3\text{H}_2$ (0.081 g, 0.5 mM), and Et_3N (0.208 mL, 1.5 mM). The reaction mixture was stirred at room

temperature for 20 h to afford deep blue solution. Blue block crystals of **2** were grown from the mother liquid after one week. Yield: 0.151 g, 52.2% based on 2-pyPzH. Elemental analysis Calc. (%) for $C_{68}H_{90}Cu_{10}N_{12}O_{26}P_6$: C, 35.31; H, 3.92; N, 7.27. Found: C, 35.23; H, 3.62; N, 7.00. IR (KBr, cm^{-1}): 3478s, 2925s, 2855m, 1610s, 1473s, 1446s, 1382s, 1188s, 1084vs, 971vs, 764s, 613m, 504m. Thermogravimetric analysis shows 3.5% weight loss from 30 to 100 °C, corresponding to the removal of four water molecules (Calcd 3.1%).

2.3. X-ray crystallographic analysis

Single crystals were selected for indexing and intensity data collection on a Rigaku SCX mini CCD diffractometer using graphite-monochromated Mo- $K\alpha$ radiation ($\lambda = 0.71073$ Å) at room temperature. A hemisphere of data was collected in the θ range 3.01–25.50° for **1** and 3.13–26.00° for **2** using a narrow-frame method with scan widths of 0.03° in ω and an exposure time of 10 s frame⁻¹. Cell parameters were refined using the program *Crystal-Clear* [12] on all observed reflections. The collected data were reduced by using *Crystal-Clear* and an absorption correction (multi-scan) was applied. The reflection data were also corrected for Lorentz and polarization effects. The structures were solved by direct methods and refined on F^2 by full matrix least squares using SHELXTL [13]. All non-hydrogen atoms were located from the Fourier maps and were refined anisotropically. All hydrogens were refined isotropically, with the isotropic vibration parameters related to the atom to which they are bonded. C15, C16, C17, C18, C19, and C20 are disordered over two sites, each with 0.5 occupancy. The H on O6 was assigned based on calculation [14]. Crystallographic and refinement details of **1** and **2** are listed in table 1. Selected bond lengths and angles are given in tables 2 and 3 for **1** and **2**, respectively. CCDC: 933674 for **1** and 933673 for **2**.

Table 1. Crystal data and structure refinements for **1** and **2**.

| Formula | $C_8H_6ClCuN_3$ | $C_{68}H_{90}Cu_{10}N_{12}O_{26}P_6$ |
|---|--------------------|--------------------------------------|
| M | 243.15 | 2312.74 |
| Crystal dimensions (mm ³) | 0.20 × 0.10 × 0.10 | 0.28 × 0.24 × 0.22 |
| Crystal system | Monoclinic | Monoclinic |
| Space group | $P2_1/c$ | $C2/m$ |
| a (Å) | 3.8368(8) | 15.4842(11) |
| b (Å) | 15.477(3) | 25.8525(12) |
| c (Å) | 14.037(3) | 13.3903(17) |
| β (°) | 93.47(3) | 110.743(3) |
| V | 832.0(3) | 5012.8(8) |
| Z | 4 | 2 |
| ρ_{Calcd} (g cm ⁻³) | 1.941 | 1.532 |
| μ (mm ⁻¹) | 2.891 | 2.241 |
| $F(0\ 0\ 0)$ | 484 | 2340 |
| Reflections collected | 7202 | 23,113 |
| Unique reflections (R_{int}) | 1551 (0.1185) | 5041 (0.009) |
| GoF on F^2 | 1.092 | 1.05 |
| R_1, wR_2^a [$I > 2\sigma(I)$] | 0.0682, 0.1053 | 0.0539, 0.1387 |
| R_1, wR_2 (all data) | 0.1232, 0.1179 | 0.0563, 0.1391 |
| $(\Delta\rho)_{\text{max}}, (\Delta\rho)_{\text{min}}$ (e Å ⁻³) | 0.371, -0.456 | 0.68, -0.66 |

$$^a R_1 = \sum ||F_o| - |F_c|| / \sum |F_o|.$$

$$wR_2 = \{ \sum w(F_o^2 - F_c^2)^2 / \sum w(F_o^2)^2 \}^{1/2}.$$

Table 2. Selected bond lengths (Å) and angles (°) for **1**.^a

| | | | |
|--------------|------------|--------------|-----------|
| Cu1–N1 | 1.995(5) | Cu1–Cl1 | 2.321(2) |
| Cu1–N2A | 1.962(5) | Cu1–Cl1B | 2.718(2) |
| Cu1–N3 | 2.057(6) | | |
| N1–Cu1–N2A | 96.6(2) | N2A–Cu1–N3 | 177.3(2) |
| N1–Cu1–N3 | 80.7(2) | N2A–Cu1–Cl1 | 92.50(16) |
| N1–Cu1–Cl1 | 159.25(16) | N2A–Cu1–Cl1B | 91.80(16) |
| N1–Cu1–Cl1B | 99.45(16) | N3–Cu1–Cl1 | 89.95(16) |
| Cu1–Cl1–Cu1C | 98.86(7) | N3–Cu1–Cl1B | 88.97(15) |

^aSymmetry code: A: 1 – x, 1 – y, 1 – z; B: 1 + x, y, z; C: x – 1, y, z.Table 3. Selected bond lengths (Å) and angles (°) for **2**.^a

| | | | |
|------------|------------|-------------|------------|
| Cu1–O2 | 1.915(3) | Cu2–O6A | 1.940(3) |
| Cu1–O4 | 2.028(3) | Cu2–N3A | 1.965(4) |
| Cu1–O5A | 2.312(4) | Cu3–O1 | 1.899(3) |
| Cu2–O3 | 1.945(3) | Cu3–O6 | 1.934(3) |
| Cu2–O4 | 1.941(3) | Cu3–N1 | 2.039(3) |
| Cu2–O6 | 2.530(3) | Cu3–N2 | 1.891(4) |
| O2–Cu1–O4 | 96.44(12) | O3–Cu2–O4 | 89.29(12) |
| O2–Cu1–O5A | 95.57(11) | O3–Cu2–O6 | 93.79(11) |
| O2–Cu1–O2C | 94.91(13) | O3–Cu2–O6A | 177.71(12) |
| O2–Cu1–O4C | 165.07(13) | O3–Cu2–N3A | 91.17(14) |
| O4–Cu1–O5A | 92.97(12) | O4–Cu2–O6 | 89.81(11) |
| O4–Cu1–O4C | 70.86(12) | O4–Cu2–O6A | 92.46(12) |
| O1–Cu3–O6 | 99.26(15) | O4–Cu2–N3A | 170.20(14) |
| O1–Cu3–N1 | 97.11(15) | O6–Cu2–O6A | 84.75(11) |
| O1–Cu3–N2 | 174.90(16) | O6–Cu2–N3A | 99.93(12) |
| O6–Cu3–N1 | 163.61(16) | O6A–Cu2–N3A | 87.36(14) |
| O6–Cu3–N2 | 84.56(16) | | |

^aSymmetry code: A: –x, y, 1 – z; B: –x, 1 – y, 1 – z; C: x, 1 – y, z.

3. Results and discussion

3.1. Syntheses

The reactions of $\text{CuCl}_2 \cdot 6\text{H}_2\text{O}$ with 2-pyPz-H and $\text{C}_6\text{H}_9\text{PO}_3\text{H}_2$ in the presence of triethylamine afforded a green solid which was recrystallized from DMF to give green crystals of $[\text{Cu}(2\text{-pyPz})\text{Cl}]$ (**1**). No phosphonate ligands are present in this compound, however pure and large crystals of **1** can only be obtained in the presence of $\text{C}_6\text{H}_9\text{PO}_3\text{H}_2$. Without adding $\text{C}_6\text{H}_9\text{PO}_3\text{H}_2$ in the reaction system, green fine powder of **1** formed. Block crystals of $[\text{Cu}_{10}(\text{OH})_4(\text{C}_6\text{H}_9\text{PO}_3)_6(2\text{-pyPz})_4]$ (**2**) formed after replacement of $\text{CuCl}_2 \cdot 6\text{H}_2\text{O}$ with CuBr_2 under the same reaction condition. In 2005, Chandrasekhar's group reported a copper cage $[\text{Cu}_{10}(\text{OH})_4(\text{t-BuPO}_3)_6(2\text{-pyPz})_4(\text{MeOH})_2]$ by reactions of $\text{Cu}(\text{ClO}_4)_2 \cdot 6\text{H}_2\text{O}$, 2-pyPzH and t-BuPO₃H₂ [15]. These results indicate that the coordination ability of counter anion and organic groups of phosphonate ligands may influence the crystallization of the final compounds.

3.2. Description of the crystal structure of $[\text{Cu}(2\text{-pyPz})\text{Cl}]$ (**1**)

Compound **1** crystallizes in monoclinic space group $P2_1/c$. The asymmetric unit consists of one Cu ion, one 2-pyPz, and one Cl^- (figure 1). Cu1 has square pyramidal geometry. The four basal positions are occupied by N1, N3, and N2A from two 2-pyPz ligands and Cl1.

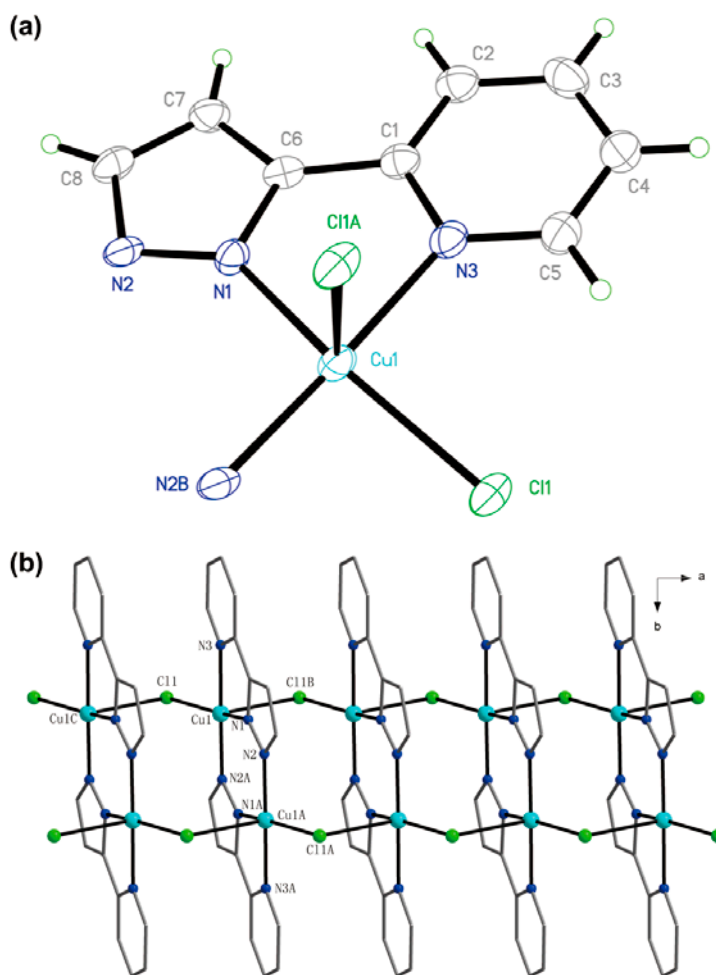
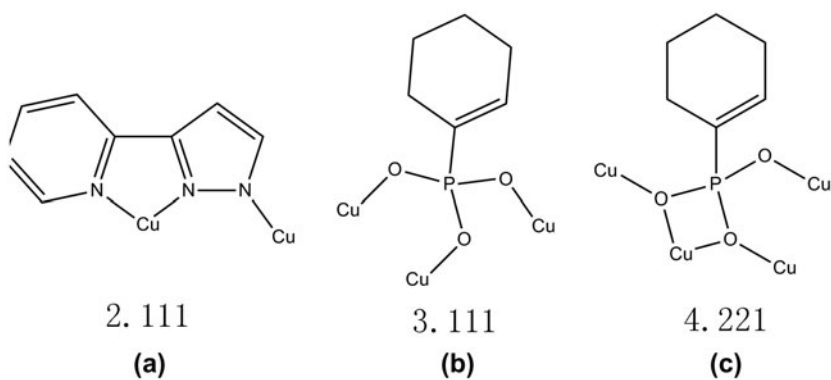
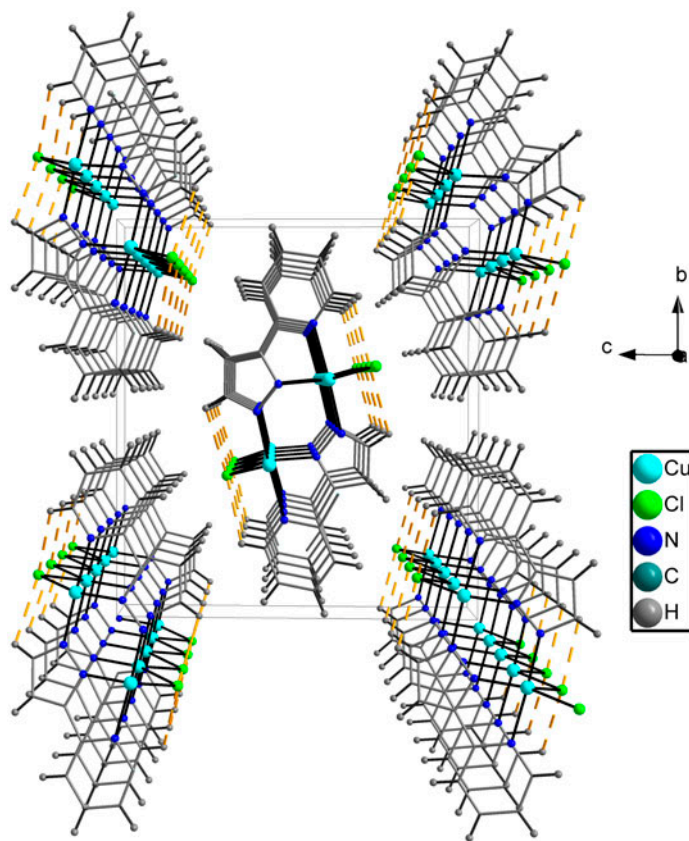


Figure 1. (a) Building unit of **1** with the atomic labeling scheme (30% probability); (b) 1-D ladder-like chain structure of **1**.

The Cu1–N distances are 1.962(6)–2.056(6) Å, close to those found in [Cu(2-pyPz)(NO₃)(H₂O)] [16]. The Cu1–Cl1 distance is 2.321(2) Å, slightly longer than that in [CuCl₂(Hppy)₂] (2.313(1) Å) [17a]. The axial position is filled with Cl1B with an elongated Cu1–Cl1B distance of 2.718(2) Å, close to that in [Cu₂Cl₂(C₅H₄NOPO₃)₂][Cu(H₂O)₆] (2.730(2) Å) [17b]. The 2-pyPz ligand serves as a chelating and bridging tridentate ligand, using its three nitrogens, thus connecting equivalent copper ions into a dimer (scheme 1) with Cu1···Cu1A distance of 3.986(1) Å. The dimers are bridged by Cl[−] along the *a*-axes into a 1-D ladder-like chain. The Cu1···Cu1C distance is 3.837(1) Å. Weak intra-molecular H-bonds (C5···Cl1 3.206(8) Å; C8···Cl1ⁱ 3.189(8) Å, *i* = 1 − *x*, 1 − *y*, 1 − *z*) were observed in this chain. In addition, π – π interactions were observed between adjacent pyridinyl groups (center to center distance is 3.837(1) Å) in the 1-D chain. These chains are packed together through van der Waals forces into a 3-D supramolecular network (figure 2).



Scheme 1.

Figure 2. 3-D network structure of **1** viewed along the *a*-axis. The weak Cl \cdots H-C interactions are shown in dashed lines.

The 1-D structure of **1** is unique when compared with other metal-2pyPz-halogen systems. [Pd(2-pyPzH)]Cl₂ [18], [Pt(2-pyPzH)]Cl₂ [19], [Au(2-pyPzH)₂]Cl [20], [RuCl₂(2-pyPzH)(DMSO)₂] [21], and [Cu(2-pyPzH)₂]Br [22] have mononuclear structures, while [Mo₂O₄(μ₂-O)Cl₂(2-pyPzH)₂] [23] has a dinuclear structure with bridging oxygen.

3.3. Description of the crystal structure of [Cu₁₀(OH)₄(C₆H₉PO₃)₆(2-pyPz)₄]·4H₂O (2·4H₂O)

Compound 2·4H₂O crystallizes in the monoclinic space group *C2/m*. It is composed of one decanuclear copper cage and four lattice waters. The cage is made up of ten copper ions, six phosphonate ligands (C₆H₉PO₃²⁻), four 2-pyPz⁻ ligands, and four OH⁻ groups (figure 3). In the asymmetric unit, there is one water disordered in four positions with each having 0.25 occupation. Cu1 has a square pyramidal geometry. The four basal positions are occupied by O2, O4, O2C, and O4C from three C₆H₉PO₃²⁻ ligands. The axial position has O5A from the third C₆H₉PO₃²⁻. The Cu1–O5A distance (2.315(5) Å) is longer than that in the basal positions (1.914(3)–2.029(4) Å), which are similar to those found in [Cu(PhCONHPO₃H)₂] (basal position Cu–O = 1.927(1)–1.965(1) Å; axial position Cu–O = 2.458(8)–2.546(9) Å) [24]. Cu2 also has a square pyramidal geometry, with O3, O4, O6A, and N3A on the basal position. The apical position is occupied by one elongated bridging O6 from μ₃-OH. The Cu2–O6 bond distance (2.532(4) Å) is longer than other Cu2–N(O) lengths (1.940(4)–1.970(4) Å). In addition, this distance is also longer than that in [Cu₁₀(OH)₄(t-BuPO₃)₆(2-pyPz)₄(MeOH)₂] (2.433(4) Å). Cu3 has a square planar geometry, coordinated with N1, N2, O1, and O6 from 2-pyPz⁻, C₆H₉PO₃²⁻, and μ₃-OH⁻. The Cu3–O lengths are 1.899(3) and

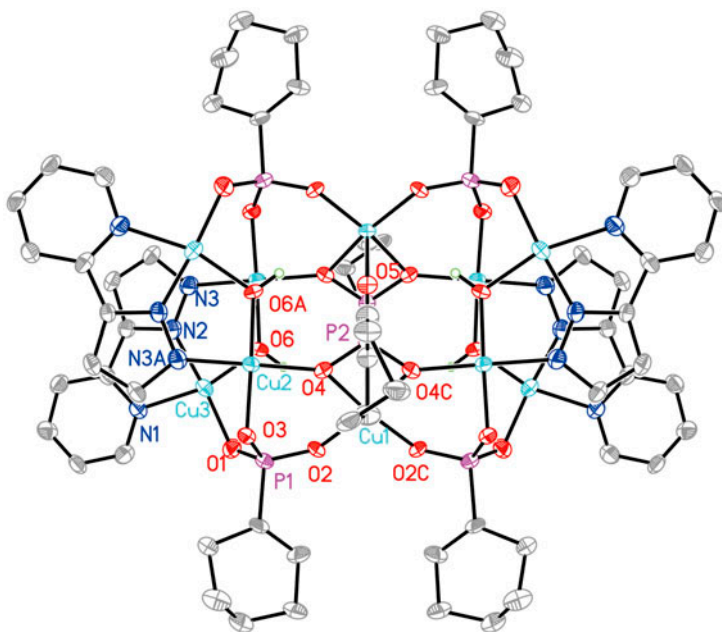


Figure 3. Molecular structure of **2** (30% probability).

1.934(3) Å, which are consistent with those in $[\text{Cu}_{10}(\text{OH})_4(\text{t-BuPO}_3)_6(2\text{-pyPz})_4(\text{MeOH})_2]$. The Cu3–N lengths are 1.891(4) and 2.039(3) Å, which are close to those in $[\text{Cu}_7(\text{O-H})_4(\text{OCH}_2\text{CF}_3)_2(\text{L})_6][\text{BF}_4]_2$ (1.958(1) and 2.097(1) Å) [25] of 1.890(4)–2.042(4) Å. The overall cage can be viewed as composed of two $\text{Cu}_4(\text{OH})_2(2\text{-pyPz})_2$ wings that are bridged by a central $\text{Cu}_2\text{P}_2\text{O}_6$ rim through phosphonate in 4.122 mode (scheme 1) [26]. The wings and the rim are further connected by four phosphonate ligands, each of which binds to three copper ions in 3.111 mode. Two copper ions are bridged by two $\text{C}_6\text{H}_9\text{PO}_3^{2-}$ ligands with the Cu1...Cu1A distance of 4.961(1) Å. In the wing, four copper ions are bridged by 2-pyPz[−] and $\mu_3\text{-OH}^-$ into a butterfly topology with Cu2...Cu3 and Cu2...Cu2A distances of 3.402(1) and 3.322(1) Å. The Cu2–O6–Cu3 bond angle is 122.69(2)°. Thus, this core structure is similar to $[\text{Cu}_{10}(\text{OH})_4(\text{t-BuPO}_3)_6(2\text{-pyPz})_4(\text{MeOH})_2]$ where t-BuPO₃[−] was employed as the linker. It should be noted that, in the latter case, one peripheral copper in each wing has an additional neutral coordinating methanol, thus with square pyramidal geometry. In **2**, the Cu in the wing position has a square planar geometry.

3.4. Magnetic properties

Variable-temperature magnetic susceptibilities of **1** and **2** were collected for a crystalline sample from 1.8 to 300 K. The χ_M and $\chi_M T$ versus T plots for **1** are shown in figure 4. At room temperature $\chi_M T$ for **1** is $0.57 \text{ cm}^3 \text{ K mol}^{-1}$, smaller than the spin-only value expected for two independent Cu(II) ions ($0.75 \text{ cm}^3 \text{ K mol}^{-1}$, $g = 2$) [11]. As the temperature is decreased $\chi_M T$ decreases steadily, reaching $0.05 \text{ cm}^3 \text{ K mol}^{-1}$ at 50 K and then continuing to decrease slowly as the temperature is lowered further. According to the structure of **1**, the magnetic exchanges between Cu(II) ions may be propagated through the $\mu\text{-N,N}$ and $\mu\text{-Cl}$ bridges. The $\mu\text{-N,N}$ bridge always transfers strong magnetic interactions. Relatively, $\mu\text{-Cl}$ plays a negligible role in propagating magnetic exchange. Thus, the susceptibility data were

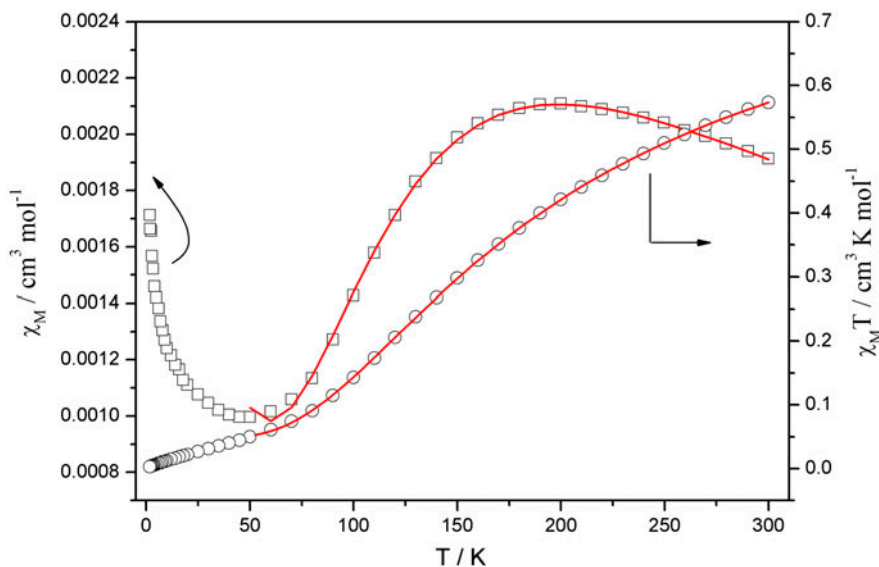


Figure 4. χ_M and $\chi_M T$ vs. T plots for **1**. Solid lines represent the best-fit.

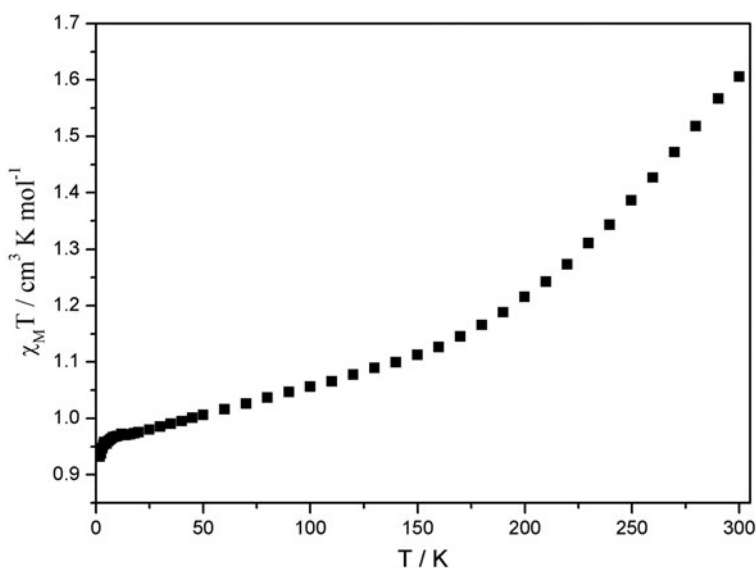


Figure 5. Plot of the susceptibility data, $\chi_M T$ vs. T for **2**.

analyzed by the Bleaney–Bowers expression based on a Heisenberg Hamiltonian $H = -2JS_1S_2$:

$$\chi_M = \frac{2Ng^2\beta^2}{kT} \frac{1}{3 + \exp(-2J/kT)} (1 - \rho) + \frac{Ng^2\beta^2}{2kT} \times \rho$$

where $2J$ is the singlet-triplet energy gap and g , β , and k have their usual meanings. ρ is a variable fraction of paramagnetic impurities [11]. Taking into account the intermolecular interactions (zj'), a good-fit resulted in the solid line in figure 4, with the parameters $g = 2.20$, $J = -119 \text{ cm}^{-1}$, $\rho = 5.4\%$, $zj' = -20 \text{ cm}^{-1}$. The value of J is a typical value for copper centers linked by bis-pyrazole bridges, for which $-240 \leq J \leq -70 \text{ cm}^{-1}$ is typically observed [15].

Figure 5 shows the $\chi_M T$ versus T plot for **2**. At 300 K, the $\chi_M T$ is $1.60 \text{ cm}^3 \text{ K M}^{-1}$, which is smaller than the spin-only value expected for non-interacting ions with $S = 1/2$ ($3.75 \text{ cm}^3 \text{ K M}^{-1}$, $g = 2$). The compound shows a rapid decrease in $\chi_M T$ at high temperature, followed by a slower decline between 180 and 8 K and then a very rapid fall below 8 K. At 1.8 K, the $\chi_M T$ is $0.92 \text{ cm}^3 \text{ K M}^{-1}$. Because of the existence of numerous exchange interactions in the cage, the fitting of the magnetic data is difficult. It is proposed that the rapid fall of $\chi_M T$ at high temperature is mainly due to the strong antiferromagnetic interaction within the $\text{Cu}_4(\text{OH})_2(2\text{-pyPz})_2$ units. The slower fall between 180 and 8 K is attributed to the combination of the above and the weaker exchange between the copper ions through phosphonate ligands. The trend of magnetic plot is very similar to that observed in $[\text{Cu}_{10}(\text{OH})_4(\text{t-BuPO}_3)_6(2\text{-pyPz})_4(\text{MeOH})_2]$ (the $\chi_M T$ at 300 and 1.8 K are 1.42 and $0.8 \text{ cm}^3 \text{ K M}^{-1}$, respectively). The similar magnetic plots of **2** and $[\text{Cu}_{10}(\text{OH})_4(\text{t-BuPO}_3)_6(2\text{-pyPz})_4(\text{MeOH})_2]$ may due to the closely related Cu–O bond distances and Cu–O–Cu bond angles.

4. Conclusion

The reaction of copper chloride and bromide with cyclohexenephosphonic acid and pyrazole ligands affords a 1-D copper polymer $[\text{Cu}(2\text{-pyPz})\text{Cl}]$ (**1**) and a decanuclear copper cage $[\text{Cu}_{10}(\text{OH})_4(\text{C}_6\text{H}_9\text{PO}_3)_6(2\text{-pyPz})_4]$ (**2**), respectively. By comparison with the layered compound $[\text{Cu}(\text{C}_6\text{H}_9\text{PO}_3)(\text{H}_2\text{O})]$ obtained under hydrothermal conditions, we can find that the reaction conditions and the counter anions play important roles in formation of the final compounds. We are trying to get new compounds by using copper salts such as $\text{Cu}(\text{ClO}_4)_2 \cdot 6\text{H}_2\text{O}$, $\text{Cu}(\text{NO}_3)_2 \cdot 3\text{H}_2\text{O}$, and $\text{CuSO}_4 \cdot 5\text{H}_2\text{O}$ to react with $\text{C}_6\text{H}_9\text{PO}_3\text{H}_2$.

Funding

This work is supported by NSFC [grant number 21201025]; NSF of Jiangsu Province [grant number BK2012643], [grant number 12KJA150001], [grant number 14KJA150001], the Six Talent Peaks project in Jiangsu Province.

Supplemental data

Supplemental data for this article can be accessed here [<http://dx.doi.org/10.1080/00958972.2015.1021342>].

References

- [1] A. Clearfield, K.D. Demadis. *Metal Phosphonate Chemistry: From Synthesis to Applications*, RSC Publishing, London (2012).
- [2] S. Maheswaran, G. Chastanet, S.J. Teat, T. Mallah, R. Sessoli, W. Wernsdorfer, R.E.P. Winpenny. *Angew. Chem. Int. Ed.*, **44**, 5044 (2005).
- [3] Y.Z. Zheng, M. Evangelisti, F. Tuna, R.E.P. Winpenny. *J. Am. Chem. Soc.*, **134**, 1057 (2012).
- [4] (a) V. Chandrasekhar, S. Kingsley. *Angew. Chem. Int. Ed.*, **39**, 2320 (2000); (b) S. Langley, M. Helliwell, R. Sessoli, S.J. Teat, R.E.P. Winpenny. *Dalton Trans.*, 3102 (2009).
- [5] (a) V. Chandrasekhar, T. Senapati, A. Dey, S. Hossain. *Dalton Trans.*, **40**, 5394 (2011); (b) V. Chandrasekhar, L. Nagarajan, S. Hossain, K. Gopal, S. Ghosh, S. Verma. *Inorg. Chem.*, **51**, 5605 (2012).
- [6] (a) E.I. Tolis, M. Helliwell, S. Langley, J. Raftery, R.E.P. Winpenny. *Angew. Chem. Int. Ed.*, **42**, 3804 (2003); (b) S. Konar, N. Bhuvanesh, A. Clearfield. *J. Am. Chem. Soc.*, **128**, 9604 (2006); (c) Y.S. Ma, Y. Song, Y.Z. Li, L.M. Zheng. *Inorg. Chem.*, **46**, 5459 (2007).
- [7] (a) Y.S. Ma, H.C. Yao, W.J. Hua, S.H. Li, Y.Z. Li, L.M. Zheng. *Inorg. Chim. Acta*, **360**, 1645 (2007); (b) H.C. Yao, Y.Z. Li, Y. Song, Y.S. Ma, L.M. Zheng, X.Q. Xin. *Inorg. Chem.*, **45**, 59 (2006).
- [8] (a) H.C. Yao, J.J. Wang, Y.S. Ma, O. Waldmann, W.X. Du, Y. Song, Y.Z. Li, L.M. Zheng, S. Decurtins, X.Q. Xin. *Chem. Commun.*, 1745 (2006); (b) Y.S. Ma, Y. Song, X.Y. Tang, R.X. Yuan. *Dalton Trans.*, **39**, 6262 (2010).
- [9] H.C. Yao, Y.Z. Li, S. Gao, Y. Song, L.M. Zheng, X.Q. Xin. *J. Solid State Chem.*, **177**, 4557 (2004).
- [10] P. Fay, H.P. Lankelma. *J. Am. Chem. Soc.*, **74**, 4933 (1952).
- [11] O. Kahn. *Molecular Magnetism*, VCH Publishers, New York (1993).
- [12] *CrystalClear*, Rigaku Corporation, Tokyo (2005).
- [13] G.M. Sheldrick. *Acta Cryst.*, **A64**, 112 (2008).
- [14] I.D. Brown, D. Altermatt. *Acta Cryst.*, **B41**, 244 (1985).
- [15] V. Chandrasekhar, L. Nagarajan, K. Gopal, V. Baskar, P. Kögerler. *Dalton Trans.*, 3143 (2005).
- [16] T.L. Hu, J.R. Li, C.S. Liu, X.S. Shi, J.N. Zhou, X.H. Bu, J. Ribas. *Inorg. Chem.*, **45**, 162 (2006).
- [17] (a) W.J. Gee, S.R. Batten. *Chem. Commun.*, **48**, 4830 (2012); (b) Y.S. Ma, T.W. Wang, Y.Z. Li, L.M. Zheng. *Inorg. Chim. Acta*, **360**, 4117 (2007).
- [18] M.D. Ward, J.S. Fleming, E. Psillakis, J.C. Jeffery, J.A. McCleverty. *Acta Cryst.*, **C54**, 609 (1998).
- [19] L. Holland, W.Z. Shen, P. von Grebe, P.J. Sanz Miguel, F. Pichierrri, A. Springer, C.A. Schalley, B. Lippert. *Dalton Trans.*, **40**, 5159 (2011).
- [20] K. Suntharalingam, D. Gupta, P.J.S. Miguel, B. Lippert, R. Vilar. *Chem. Eur. J.*, **16**, 3613 (2010).
- [21] Í. Ferrer, J. Rich, X. Fontrodona, M. Rodríguez, I. Romero. *Dalton Trans.*, **42**, 13461 (2013).

- [22] J.S. Uber, Y. Vogels, D. Helder, I. Mutikainen, U. Turpeinen, W.T. Fu, O. Roubeau, P. Gamez, J. Reedijk. *Eur. J. Inorg. Chem.*, 4197 (2007).
- [23] A.C. Coelho, M. Nolasco, S.S. Balula, M.M. Antunes, C.C.L. Pereira, F.A. Almeida Paz, A.A. Valente, M. Pillinger, P. Ribeiro-Claro, J. Klinowski, I.S. Gonçalves. *Inorg. Chem.*, **50**, 525 (2011).
- [24] R. Murugavel, M.P. Singh. *Inorg. Chem.*, **45**, 9154 (2006).
- [25] J.J. Henkelis, L.F. Jones, M.P. de Miranda, C.A. Kilner, M.A. Halcrow. *Inorg. Chem.*, **49**, 11127 (2010).
- [26] R.A. Coxall, S.G. Harris, D.K. Henderson, S. Parsons, P.A. Tasker, R.E.P. Winpenny. *J. Chem. Soc., Dalton Trans.*, 2349 (2000).